THE JOURNAL OF PHYSICAL CHEMISTRY C

Article

Cite This: J. Phys. Chem. C 2018, 122, 18562−18569

pubs.acs.org/JPCC

Bromide Adsorption on Pt(111) over a Wide Range of pH: Cyclic Voltammetry and CO Displacement Experiments

Gisele A. B. Mello,[†,‡] Valentín Briega-Martos,[†] Víctor Climent,*[,†] and Juan M. Feliu*[,†]

[†]Instituto de Electroquímica, Universidad de Alicante, Apartado 99, E-03080 Alicante, Spain

[‡]Curso de Licenciatura em Química, Instituto de Ciências da Educação, Universidade Federal do Oeste do Pará, Avenida Marechal Rondon, s/n, CEP 68040-070, Santarém, PA, Brazil

ABSTRACT: Bromide adsorption on Pt(111) is investigated by means of cyclic voltammetry and CO displacement experiments at different pH values. In acidic pH, bromide adsorption is strongly overlapped with hydrogen desorption process. However, as the pH increases, hydrogen adsorption process displaces toward negative potentials while bromide adsorption remains nearly in the same potential region. In consequence, both processes decouple at higher pH values. The structural transition from Pt(111)-(1×1) to Pt(111)-(3×3)-4Br is pH independent, in the SHE scale, and not observed for pH > 9.1. Values of pztc are extracted from the combination of voltammetric and CO displaced charges. An alternative approach to obtain charge curves is based on the coincidence of the curves at the structural transition characteristic of the bromide adlayer completion. Pztc values obtained from different approaches with and without bromide are compared, and their dependence on pH discussed. A thermodynamic analysis is carried out to obtain hydrogen Gibbs excess and charge number from the Esin Markov analysis.

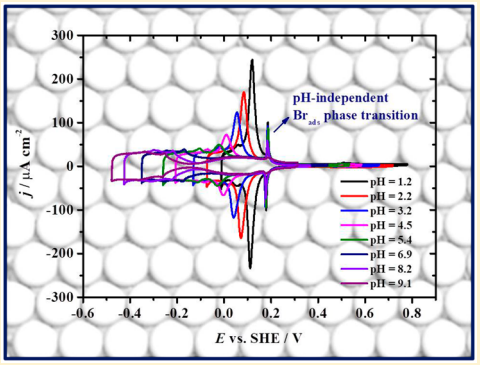

1. INTRODUCTION

The knowledge of the properties of the metal−electrolyte interface has fundamental importance in electrochemistry. It is well established that the rate-determining step of all electrocatalytic reactions necessarily involves adsorbed species or at least a specific interaction between reactants or intermediates and the electrocatalytic surface. Such interactions are expected to be extremely sensitive to the interfacial charge and/or the existence of coadsorption phenomena. For that reason, quantifying the amount of charge separation at the electrochemical double layer is extremely important to rationalize the electrocatalytic phenomena. For this, the fundamental property that should be investigated to relate the electrode potential, which is the directly measurable quantity, with the interfacial charge, is the potential of zero charge (pzc).[1−5] Two different types of pzc can be defined at platinum electrodes, the potential of zero free charge (pzfc) and the potential of zero total charge (pztc). While the free charge considers the true electronic excess charge on the metal, compensated by the ionic charge on the electrolyte, the only accessible quantity is the total charge which includes both capacitive and pseudocapacitive (faradaic) contributions. The pztc can be measured with the CO displacement experiments,[1,2,4−9] while the pzfc can only be calculated in some particular cases from the pztc by using some additional assumptions.[10] Besides this, the location of the pzfc can be inferred from some indirect measurements like the reorientation of interfacial water molecules monitored by laser-induced temperature jump experiments.[11−13]

When anion specific adsorption takes place on the electrode surface, it is extremely important to determine the charge transfer characteristics involved in this process, since it implies changes in the pztc and it also promotes electrode surface modifications.[3,14] The structural adlayer of the adsorbed anion can be "incommensurate" or "commensurate" depending on what type of interaction is stronger, as pointed out by Lucas et al.[15] On the one hand, if the interaction between nearby adatoms is stronger, the structural adlayer will be "incommensurate". On the other hand, if the adatom-substrate interaction is stronger, the structural adlayer will be "commensurate".

Bromide adsorption on Pt(111) was subject of investigation by Hubbard's group[16−18] providing precious information about the characterization of the formed adlayers. UHV measurements by LEED and Auger spectroscopy were employed to characterize the adlayer, and these works opened the way for further similar investigations.[3,19−22] The Pt(111)-Br$_{ads}$ adlayer was also characterized by STM[3,23] and surface X-ray scattering.[19] The bromide adlayers can be formed either from bromide solutions or bromide vapors.[3] A structural transition at 0.25 V vs RHE in 0.1 M $HClO_4$ was observed.[3,18,23] It was first proposed that this feature corresponds to the change from a Pt(111)-(3×3)-4Br adlattice at high potentials to a Pt(111)-(4×4)-7Br adlattice at low

Received: June 14, 2018
Revised: July 10, 2018
Published: July 23, 2018

DOI: 10.1021/acs.jpcc.8b05685
J. Phys. Chem. C 2018, 122, 18562−18569

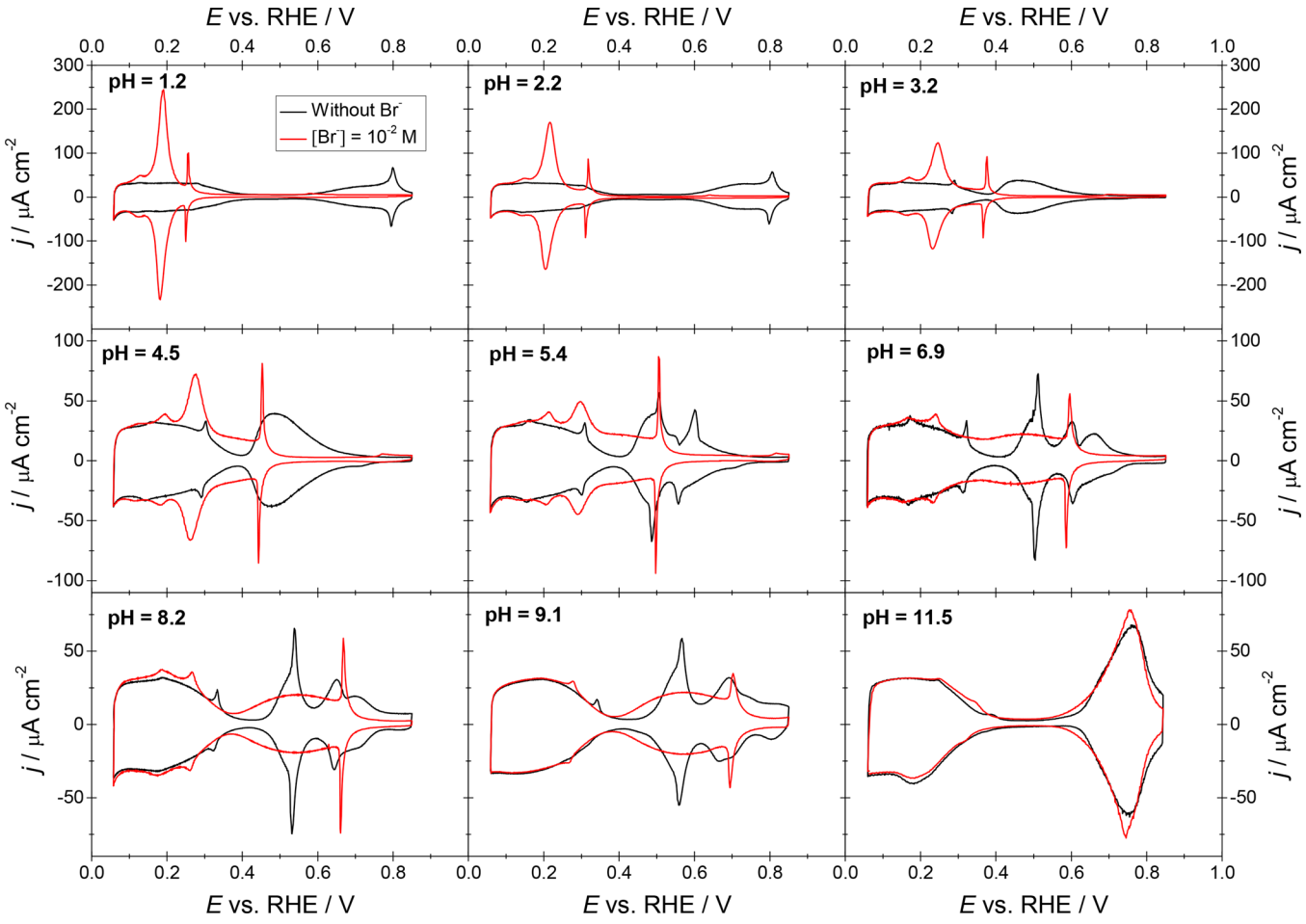

Figure 1. Voltammetric profiles for Pt(111) in different solutions with pH values ranging from 1.2 to 11.5 in the absence of KBr (black line) and in the presence of 10^{-2} KBr (red line). Scan rate: 50 mV s^{-1}.

potentials,[18] but Itaya et al. observed an incommensurate Pt(111)-(1×1) structure instead of Pt(111)-(4×4)-7Br.[23] Independently of the technique used for the characterization of the Pt(111)-Br_{ads} adlayer, it was shown that the Pt(111)-(3×3)-4Br structure is dense and the bromine adatoms are arranged in a closed-packed hexagonal layer, where the Br−Br distance is close to the van der Waals diameter of bromine. It was also pointed out that these adlayers are ordered preferentially along the directions of the substrate densest rows.[3,16−18,24] Lucas et al.[19] proposed similar observations, although in these studies they observed that the (3×3) adlayer structure was incommensurate, whereas Orts et al.[3] proposed it as commensurate.

In the present work, the knowledge about bromide adsorption on Pt(111) is extended by performing cyclic voltammetry and CO displacement experiments in solutions with a wide range of pH values.

2. EXPERIMENTAL SECTION

Experiments were performed in a glass electrochemical cell with three electrodes following the general procedure described in Korzeniewski et al.[25] The Pt(111) working electrode was prepared from a small Pt bead ca. 2 mm in diameter according to the procedure described by Clavilier et al.[26] The reference electrode was a reversible hydrogen electrode (RHE) in all cases, although some results are presented vs the SHE in some figures. The counter electrode was a platinum coiled wire cleaned by flame annealing and quenched with ultrapure water.

Working solutions with pH values lower than 3 were prepared by using $HClO_4$ (Merck, for analysis) and $KClO_4$ (EMSURE ACS for analysis 99.5%−100.5%, Merck). For pH values ranging from 3 to 9, phosphate buffer solutions were employed (Na_2HPO_4 and NaH_2PO_4, traceSELECT, Fluka Analytical). Alkaline solutions were prepared with NaOH (99.99%, trace metals, Sigma-Aldrich) and $KClO_4$. Bromide adsorption was investigated by using KBr (Merck, Suprapur, 99.99%). Ultrapure water (Elga PureLab Ultra, 18.2 MΩ cm) was employed for glassware cleaning and preparation of all the working solutions. Ar, H_2, and CO (N50, Air Liquide) were also employed. CO displacement experiments were performed as described elsewhere.[4,7−9]

The electrode potentials were controlled using a waveform generator (PARC 175, EG&G) together with a potentiostat (eDAQ 401) and a digital recorder (eDAQ ED401). All the experiments were carried out at room temperature.

3. RESULTS AND DISCUSSION

Bromide Adsorption on Pt(111). Cyclic voltammetric profiles for Pt(111) in the absence of bromide and in the presence of 10^{-2} M Br^- at pH values from 1.2 to 11.5 are shown in Figure 1. In the case of the blank voltammetries without bromide, the hydrogen adsorption/desorption region appears between 0.06 and 0.4 V (vs RHE) for all the

DOI: 10.1021/acs.jpcc.8b05685
J. Phys. Chem. C 2018, 122, 18562−18569

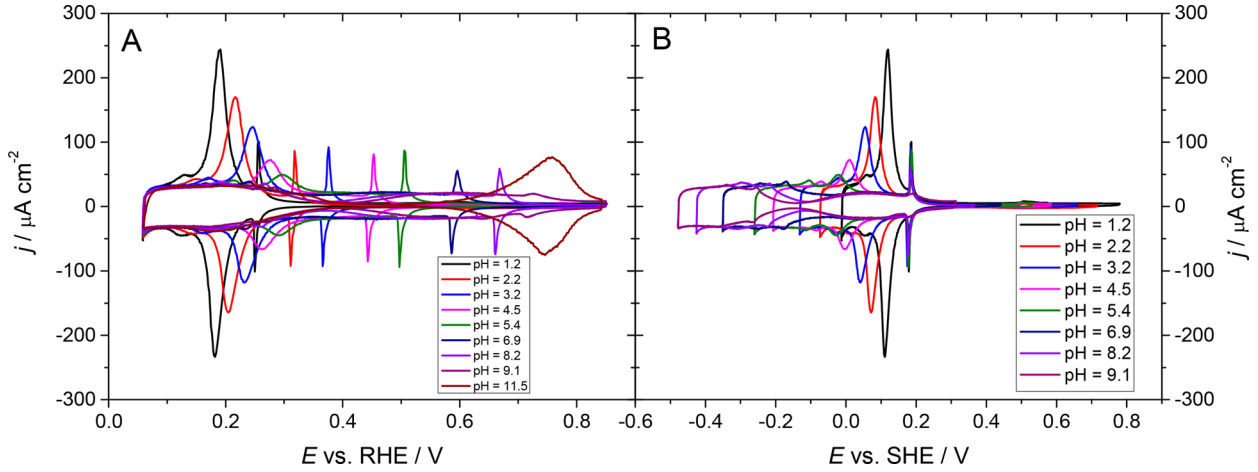

Figure 2. Voltammetric profiles for Pt(111) in different solutions with pH values ranging from 1.2 to 11.5 in the presence of 10^{-2} M KBr in the RHE scale (A) and in the SHE scale (B). Scan rate: 50 mV s^{-1}.

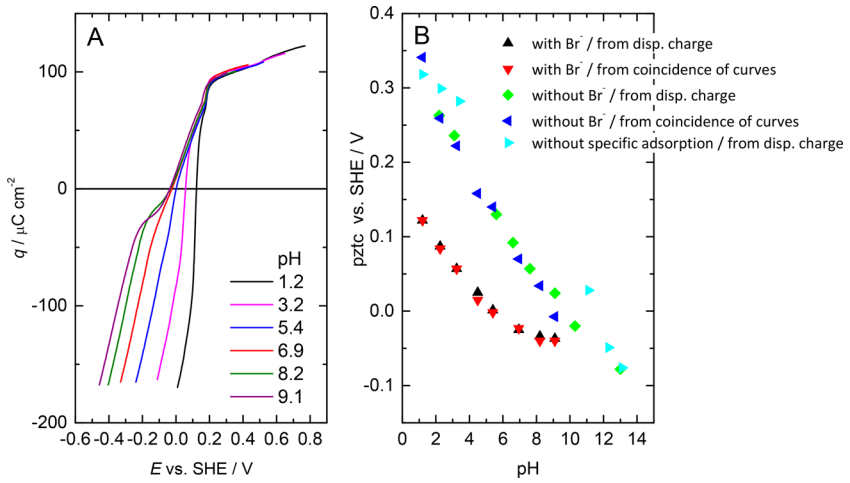

Figure 3. Charge curves obtained from the integration of the corresponding voltammograms with 10^{-2} M KBr and using the charge obtained by CO displacement at 0.1 V as the integration constant (A) and comparison of the potential of zero charge at different pH values for different compositions (B).

experiments in the complete pH range investigated.[27−29] However, the voltammetric peaks associated with the (100) and (110) defects shift with pH with a non-Nernstian behavior.[28,29] Such shift has been recently attributed to the presence of cations in the buffer solution.[30] When no anion specific adsorption is present, the adsorption/desorption feature of hydroxyl anions is observed at high potentials, while in the presence of phosphate anions this region is displaced to more negative potentials and different irreversible sharp peaks appear due to the adsorption of phosphate species.[28] It is important to take into account that the pK_a for the phosphate species at the metallsolution interface are much lower than their values for the same species in the bulk solution.[31] Therefore, phosphate species that would not be found in the bulk solution at a certain pH could be present at the interface.

In the presence of 10^{-2} M KBr, the voltammetric profiles are significantly different because of the specific adsorption of bromide anions.[3,7,9] Symmetrical curves are obtained in both positive and negative-going sweeps for all the pH values. In the case of 0.1 M $HClO_4$ (pH = 1.2) most of the voltammetric charge appears at potentials lower than 0.4 V vs RHE, and two main peaks can be observed at 0.18 and 0.23 V vs RHE.[3] The measured charges at low potentials arise from both hydrogen adsorption/desorption and bromide desorption/adsorption on the platinum surface.[15,20,22] In acid solutions, these processes overlap significantly,[3] but, as the pH increases, the bromide adsorption moves to more positive potential values (in the RHE scale), separating from the hydrogen adsorption/desorption region. Bromide adsorption can also be inferred by the suppression of the OH^- desorption/adsorption region, as observed for other specifically adsorbed anions.[5,32] This feature is completely suppressed at acidic pH values, but, as the solution pH is increased, the adsorption strength of bromide anions decreases, and, for pH = 11.5, the hydroxyl anions desorption/adsorption region remains practically unchanged.[18,22] In addition, the first peak associated with bromide adsorption becomes broader and diminishes drastically its intensity as the pH of the solution is increased, which indicates that the adsorption strength of Br^- is decreasing.

The sharp peak at 0.18 V vs RHE at pH = 1.2 is associated with the structural transition from Pt(111)-(1×1) (or Pt(111)(4×4)-7Br) to Pt(111)(3×3)-4Br (in the positive-going scan), which involves the oxidative adsorption of Br^- and the reconstruction of the bromide adlattice.[3,16−18,23,24] It is important to remark that the peak potential of this spike is

DOI: 10.1021/acs.jpcc.8b05685
J. Phys. Chem. C 2018, 122, 18562−18569

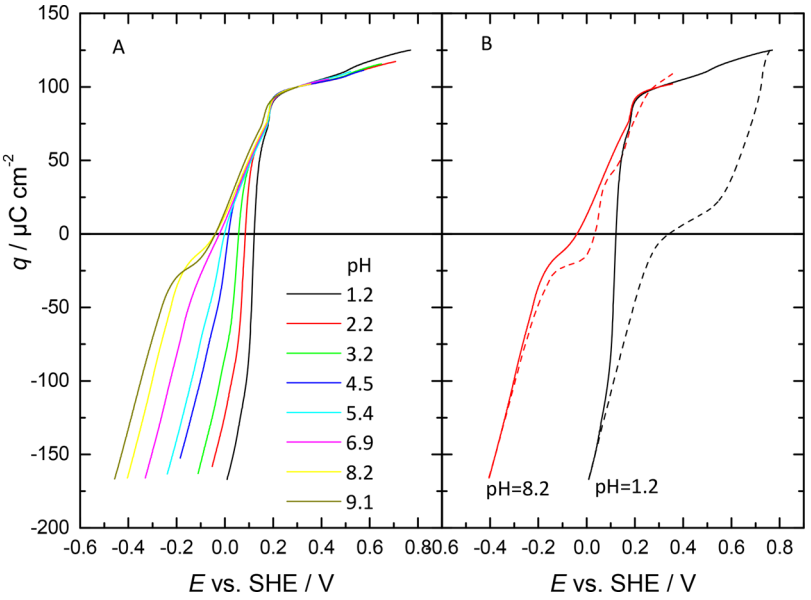

Figure 4. Charge curves obtained from the integration of the corresponding voltammograms with 10^{-2} M KBr and from the coincidence of the curves (A). Exemplification of the method employed to establish the relative position of charge curves (i.e., integration constant) from the coincidence with (solid lines) and without (dashed lines) bromide in the low potential region (at 0.1 V vs RHE) (B).

pH independent in the SHE scale (as can be seen in Figure 2), suggesting that this structural transition does not involve the displacement of hydrogen.[18,22] This reconstruction peak becomes markedly broader and lower at pH = 9.1, while at pH = 11.5 completely vanishes. This reinforces the idea that bromide adsorption is strongly inhibited by the competitive adsorption of OH_{ads}. In this sense, pH = 9.1 would be the pH limit in which bromide anions could adsorb promoting the structural transition (Figure 2). The pH-independent behavior of the structural transition spike for bromide differs from H_2SO_4 solutions because in the latter case the adsorption of sulfate also implies the transfer of protons.[33]

The curves plotting the total charge as a function of potential for some of the studied pH values are shown in Figure 3A. These curves were obtained from the integration of the cyclic voltammogram in the presence of bromide using the total charge obtained from CO displacement experiments performed at 0.1 V vs RHE as the integration constant.[1,5,34] Displaced charges with CO were corrected to consider the remaining charge on the interface after CO adsorption.[35] From these plots, the potential of zero total charge (pztc) can be estimated as the point where the curve crosses the potential axis, i.e. the potential value at $q = 0$.[2,34,36,37] As usual, there is an increase in the charge densities with potential (Figure 3A). The negative charge at lower potentials is mainly due to the reductive hydrogen adsorption. The inflection points mark the potential range where bromide adsorption takes place. The first inflection at lower potentials (overlapped with the hydrogen adsorption process) marks the onset of bromide adsorption while the one at higher potentials similar in shape to sulfate adsorption, marks the completion of the adlayer, which finishes in the sharp spike, except for pH 9.1 in which the sharp spike is nearly absent. The positive charges above 0.12 V in the most acidic solution are associated with the dominance of the oxidative adsorption of bromide species. At increasing pH, the slope of the charge/potential profiles decreases, demonstrating the separation of bromide adsorption process as a function of pH: in more acidic solutions the bromide adsorption occurs in a competitive process with hydrogen desorption and increasing the pH the bromide adsorption occurs at higher relative potentials, on a surface almost free of adsorbed hydrogen, where mainly water is in contact with the metal. Figure 3B shows a comparison between the pztc values for phosphate buffer solutions in presence and in absence of bromide. Note that increasing the pH, the pztc values are shifted toward less positive values when 10^{-2} M Br^- is present, which indicates that in acid medium bromide adsorption is stronger than in alkaline medium. The bromide structural transition takes place at higher potentials than the pztc for all cases. It is noteworthy that the ptzc for pH 6.9 and 9.1 are very close, although the bromide adsorption in pH 9.1 is strongly inhibited in comparison to pH 6.9. This indicates that pH 9.1 seems to be the pH limit in which the competition with the adsorption of oxygenated species prevents these surface phenomena promoted by bromide. In the absence of bromide anions, a monotonic trend is observed, since different phosphate species are participating depending on the pH. However, it can be seen that the pztc always tends to approach the value corresponding to the absence of specific anion adsorption at very high pH (Figure 3B).

It is important to highlight that, in the presence of strongly adsorbed anions, the interfacial properties at the highest potential range should be pH independent, since the adsorption of oxygenated species is suppressed by anion adsorption (Figure 1). Hence, in the particular region where the Br^- adlayer is completed, no other contributions are involved and the charge at the interface should be pH independent.[32] The coincidence of the voltammetric curves between 0.12 and 0.17 V (vs SHE) in the pH range between 3.4 and 9.1 (Figure 2) illustrates this idea. Also, the charge curves in Figure 3A demonstrate the independence of the interfacial properties on pH in the highest potential range. It must be remarked that this is obtained as an experimental result from the combination of current integration and displaced charges. An alternative approach would be to impose the coincidence of the curves at a potential higher than the

DOI: 10.1021/acs.jpcc.8b05685
J. Phys. Chem. C 2018, 122, 18562−18569

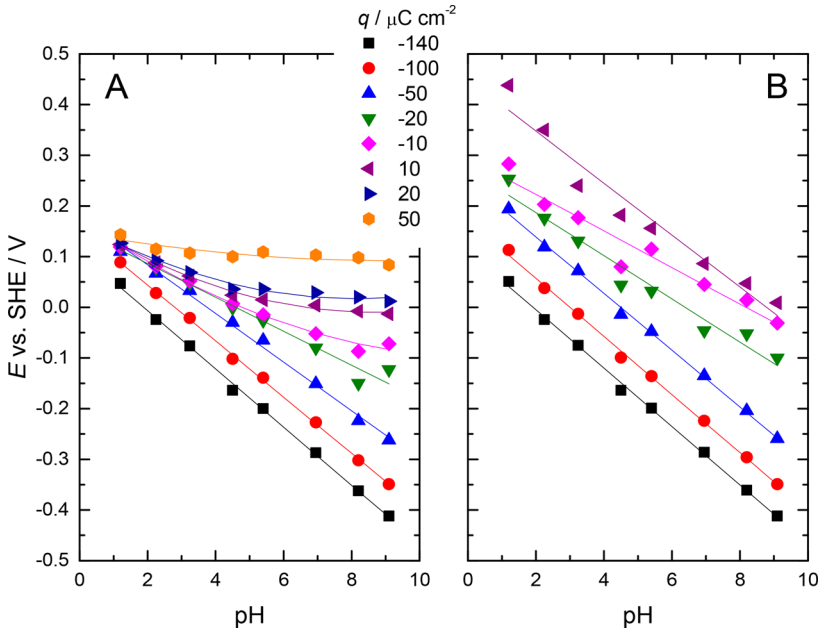

Figure 5. Plot of potential of constant charge as a function of pH for solutions with (A) and without (B) bromide. The lines represent the best fit to either a straight line or to a parabola (with bromide for $q > -16$ μC cm^{-2}).

spike at 0.15 V. In this way, the relative position of the charge curves could be elucidated without the use of CO displaced charges as integration constant. We would only need one integration constant for one of the curves to obtain the absolute position of all the curves at the different pHs. On the other hand, charge curves with and without bromide should coincide in the lowest potential range where bromide is completely desorbed and the properties of the interphase are dominated by hydrogen adsorption. This is illustrated in Figure 4. In this figure all the curves integrated from the voltammograms with bromide in different pH solutions are adjusted to coincide at 0.3 V SHE. Then, every curve recorded in the absence of bromide is made to coincide with the corresponding curve recorded at the same pH but with bromide at 0.1 V RHE (this potential shifts in the SHE scale). In this way, the relative position of all the curves is adjusted. Finally, one single integration constant would only be needed to adjust the absolute position of all the curves with and without bromide and for every pH. This integration constant has been taken as -154 μC cm^{-2} at 0.1 V RHE for pH = 1.2. This number corresponds to a displaced charge of -141 μC cm^{-2} plus a correction due to the remaining charge on the CO covered surface after the displacement experiment of -13 μC cm^{-2}.

In this way, the dependence of pztc values with pH can be accurately obtained with less experimental uncertainty than the one associated with the CO displacement. It should be stressed that one of the uncertainties associated with the CO displacement, the dependence of the correction for the remaining charge on the CO covered surface with the pH, is avoided in this approach since only one integration constant is used at a single pH value. The same approach has been previously used to obtain information on the interfacial properties in a much narrow pH range.[32,38] From the result plotted in Figure 4, the pztc values for solutions with and without bromide can be easily obtained from the intersection with the $q = 0$ axis. The results obtained with this approach are plotted in Figure 3B, together with the values obtained with the charge displacement technique, demonstrating the good agreement between both approaches. Because the accuracy in the determination of the relative position of the curves is better with this second approach, we adopt it for the analysis that follows.

The plot of pztc vs pH is a particular case of an Esin Markov plot. In general, the Esin Markov coefficient is defined as the variation of the potential at constant charge as a function of the chemical potential of one species in solution. Under the light of the electrocapillary equation this can be related with the formal charge transfer number at constant charge:

$$d\xi = E\ dq - \Gamma d\mu_{H^+} \tag{1}$$

Here ξ is the Parsons function defined as $\xi = \gamma + qE$. According to this exact differencial, based on the equality of cross partial derivatives, we obtain the desired relationship:

$$\left(\frac{\partial E}{\partial \mu_{H^+}}\right)_q = -\frac{1}{RT\ \ln 10}\left(\frac{\partial E}{\partial pH}\right)_q = -\left(\frac{\partial \Gamma_{H^+}}{\partial q}\right)_\mu \tag{2}$$

Here

$$n' = -\frac{1}{F}\left(\frac{\partial q}{\partial \Gamma_{H^+}}\right)_\mu = -\frac{RT\ \ln 10}{F}\left(\frac{\partial E}{\partial pH}\right)_q^{-1} \tag{3}$$

is the formal partial charge number for H^+ adsorption.

From the curves of Figure 4A, we can take horizontal cuts to obtain values of potential for different values of constant charge to plot them as a function of the pH. The result is shown for some selected charge value in Figure 5, parts A and B, for solutions with and without bromide, respectively.

From the slope of the plots, the charge numbers involved in the adsorption of hydrogen can be calculated. For the curves obtained in the presence of bromide, at charges higher than -16 μC cm^{-2} the plots clearly deviates from straight lines and a parabolic fit was used to extract the slopes. Such deviation from linearity in a consequence of the coadsorption of bromide

DOI: 10.1021/acs.jpcc.8b05685
J. Phys. Chem. C 2018, 122, 18562−18569

with hydrogen, since the degree of the overlap of both processes changes with pH. In this way, for charges above −20 μC cm^{-2}, while hydrogen adsorption process is already finished in the curves with highest pH, there is still a pH dependence for the curves with lowest pH. Regarding the plot in the absence of bromide the plot shows parallel straight lines, indicating that the charge numbers in this case are relatively insensitive to either pH or charge (potential).

The charge numbers calculated in this way are plotted as a function of the charge in Figure 6:

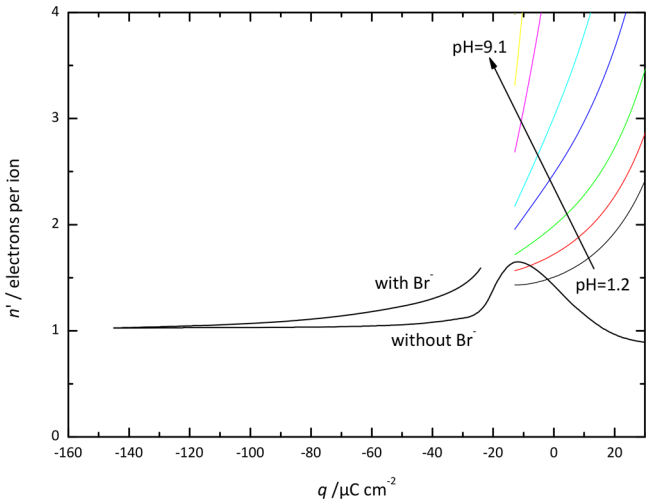

Figure 6. Charge numbers at constant chemical potential obtained from the inverse of Esin Markov coefficient plotted as a function of the charge. To obtain the slopes from the curves with bromide, linear fits are used for $q < -20$ μC cm^{-2} and quadratic fit for $q > -20$ μC cm^{-2}.

Charge numbers involved in hydrogen adsorption in the absence of bromide are very close to one in accordance with previous calculations.[39] This suggests that H^+ ions are totally discharged upon adsorption. In the case of solutions that contain bromide, the charge number tends to one at the lowest charge (potential) values but small deviations from unity take place. This reflects the coadsorption effect of bromide as has been demonstrated before for other anions. In the presence of coadsorption:

$$n' = -\frac{1}{F}\left(\frac{\partial q}{\partial \Gamma_H}\right)_{\mu_{H^+}} = -\frac{1}{F}\left(\frac{\partial q}{\partial \Gamma_H}\right)_{\mu_{H^+},\Gamma_{Br}} - \frac{1}{F}\left(\frac{\partial q}{\partial \Gamma_{Br}}\right)_{\mu_{H^+},\Gamma_H}\left(\frac{\partial \Gamma_{Br}}{\partial \Gamma_H}\right)_{\mu_{H^+}} \quad (4)$$

Since $\left(\frac{\partial q}{\partial \Gamma_{Br}}\right)_{\mu_{H^+},\Gamma_H}$ is always positive, for the adsorption of an anion, $\left(\frac{\partial \Gamma_{Br}}{\partial \Gamma_H}\right)_{\mu_{H^+}}$ must be negative, as corresponds to a competitive adsorption phenomena.

Additional information can be obtained from eq 1. According to this equation, the hydrogen coverage, Γ_{H^+}, can be obtained by differentiating ξ:

$$\Gamma_H = -\left(\frac{\partial \xi}{\partial \mu_{H^+}}\right)_q = \frac{1}{RT \ln 10}\left(\frac{\partial \xi}{\partial pH}\right)_q \quad (5)$$

Values of ξ can be obtained from integration of the potential as a function of charge, except for an integration constant. Although this integration constant is unknown, it can be assumed independent of the pH at sufficiently high potential (charge) values. Following this approach, the potential was integrated as a function of charge and all the resulting curves were shifted to make them coincide at $q = 100$ μC cm^{-2}. The result is shown in Figure 7:

According to eq 5 hydrogen coverage can be obtained from the slopes of plots in Figure 7B. Although these plots are nearly linear they exhibit some curvature, especially those at higher charge, indicating that the low coverages of hydrogen depend slightly on pH. For this reason, both quadratic and linear fits were used to extract the slopes and the results are compared in Figure 8.

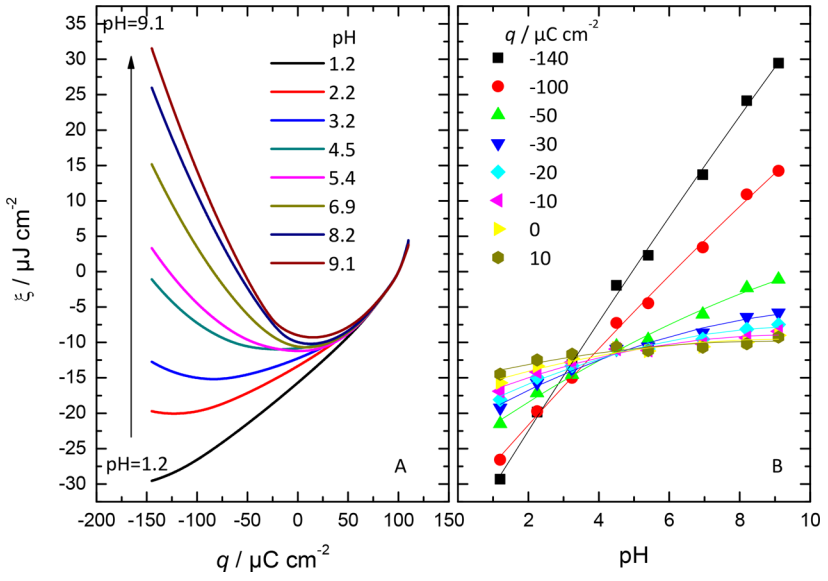

Figure 7. Plot of Parsons function, ξ, (A) as a function of charge for different pH or (B) as a function of pH for different values of charge, as integrated for the solutions containing bromide.

DOI: 10.1021/acs.jpcc.8b05685
J. Phys. Chem. C 2018, 122, 18562−18569

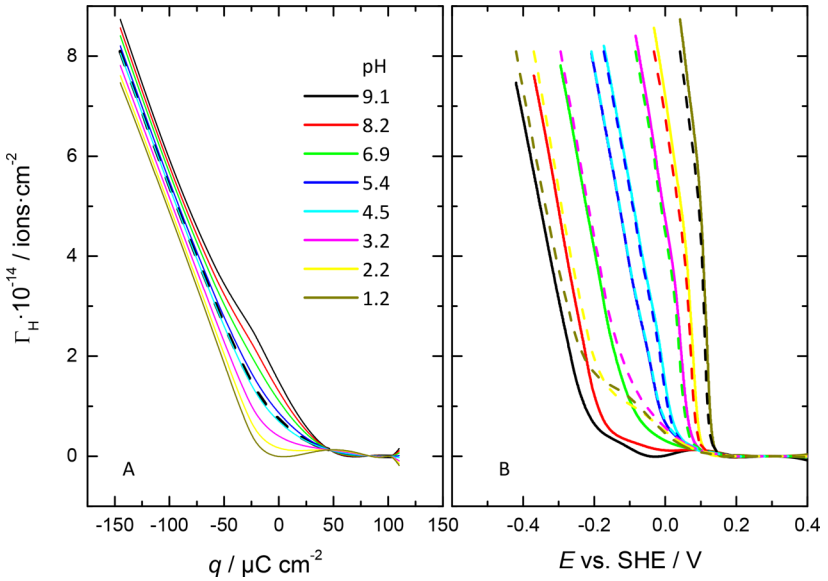

Figure 8. Plot of the surface excess as a function of (A) charge and (B) potential. Dashed lines correspond to the result obtained with a linear fit, while solid lines are results obtained with quadratic fit.

The maximum hydrogen coverage obtained is around 8.5 × 10^{14} cm^{-2} what is equivalent to 136 μC cm^{-2} in reasonable agreement with the value obtained with voltammetry. While there is little difference between the quadratic and linear fit for high coverage values, at low coverages, the results from the quadratic fit seem to produce better results. It is also noteworthy the change of slope in the curves for the lower pH in Figure 8B, which signals the potential where bromide adsorption forces the displacement of the remaining adsorbed hydrogen.

4. CONCLUSIONS

In this work, the adsorption of bromide adlayers on Pt(111) at different pH values is studied. Results show that when bromide anions are present, the same results are obtained independently of the presence of other possible species that could adsorb specifically, such as phosphate or sulfate anions. It is observed that the sharp peak from the structural transition from Pt(111)-(1×1) to Pt(111)-(3×3)-4Br is pH independent and pH = 9.1 seems to be the limit in which the adsorption of oxygenated species does not prevent this surface reconstruction. CO displacement experiments point out that the pztc is displaced to more negative values as the pH is increased, indicating that bromide adsorption is stronger in acid than in alkaline media.

Charge curves have been obtained from an alternative method based on the coincidence of charge for all pH solutions at the potential where the bromide adlayer is complete (at 0.3 V vs SHE). In this way, the curves with and without bromide for different pH solutions can be compared. The result is in excellent agreement with that obtained from CO displacement and overcomes the uncertainty inherent to the latter technique regarding the remaining charge on the CO covered surface. The thermodynamic analysis allowed calculation of hydrogen coverage and charge number under different pH conditions. The Esin Markov analysis signals the coadsorption of bromide and hydrogen and that the degree of overlap of both processes changes with pH.

AUTHOR INFORMATION

Corresponding Authors

*(V.C.) E-mail: victor.climent@ua.es.
*(J.M.F.) E-mail: juan.feliu@ua.es.

ORCID

Víctor Climent: 0000-0002-2033-5284

Notes

The authors declare no competing financial interest.

ACKNOWLEDGMENTS

This work has been financially supported by the MCINN-FEDER (Spain) through Project CTQ2016-76221-P. V.B.-M. thankfully acknowledges to MINECO the award of a predoctoral grant (BES-2014-068176, Project CTQ2013-44803-P). G.A.B.M. expresses thanks for the postdoctorate fellowship from CNPq (Grant No. PDE 233268/2014-6).

REFERENCES

(1) Cuesta, A. Measurement of the surface charge density of CO-saturated Pt(111) electrodes as a function of potential: The potential of zero charge of Pt(111). *Surf. Sci.* **2004**, *572*, 11−22.
(2) Climent, V.; Gómez, R.; Feliu, J. M. Effect of increasing amount of steps on the potential of zero total charge of Pt(111) electrodes. *Electrochim. Acta* **1999**, *45*, 629−637.
(3) Orts, J. M.; Gómez, R.; Feliu, J. M.; Aldaz, A.; Clavilier, J. Nature of Br adlayers on Pt(111) single-crystal surfaces. Voltammetric, charge displacement, and ex situ STM experiments. *J. Phys. Chem.* **1996**, *100*, 2334−2344.
(4) Rizo, R.; Sitta, E.; Herrero, E.; Climent, V.; Feliu, J. M. Towards the understanding of the interfacial pH scale at Pt(111) electrodes. *Electrochim. Acta* **2015**, *162*, 138−145.
(5) Martínez-Hincapié, R.; Sebastián-Pascual, P.; Climent, V.; Feliu, J. M. Exploring the interfacial neutral pH region of Pt(111) electrodes. *Electrochem. Commun.* **2015**, *58*, 62−64.
(6) Clavilier, J.; Orts, J. M.; Gómez, R.; Feliu, J. M.; Aldaz, A. *On the Nature of the Charged Species Displaced by CO Adsorption from Platinum Oriented Electrodes in Sulphuric Acid Solution*; Conway, B. E., Jerkiewicz, G., Eds.; The Electrochemical Society, INC.: Pennington, NJ, 1994; Vol. *94−21*; pp 167−183.
(7) Orts, J. M.; Gómez, R.; Feliu, J. M.; Aldaz, A.; Clavilier, J. Potentiostatic charge displacement by exchanging adsorbed species on

DOI: 10.1021/acs.jpcc.8b05685
J. Phys. Chem. C 2018, 122, 18562−18569

Pt(111) electrodes—acidic electrolytes with specific anion adsorption. *Electrochim. Acta* **1994**, *39*, 1519−1524.
(8) Clavilier, J.; Albalat, R.; Gómez, R.; Orts, J. M.; Feliu, J. M.; Aldaz, A. Study of the charge displacement at constant potential during CO adsorption on Pt(110) and Pt(111) electrodes in contact with a perchloric acid solution. *J. Electroanal. Chem.* **1992**, *330*, 489−497.
(9) Clavilier, J.; Albalat, R.; Gómez, R.; Orts, J. M.; Feliu, J. M. Displacement of adsorbed iodine on platinum single-crystal electrodes by irreversible adsorption of CO at controlled potential. *J. Electroanal. Chem.* **1993**, *360*, 325−335.
(10) Climent, V.; Gómez, R.; Orts, J. M.; Aldaz, A.; Feliu, J. M. *The potential of zero total charge of single-crystal electrodes of platinum group metals*; The Electrochemical Society, Inc.: Pennington, NJ, 1997; Vol. *97−17*; pp 222−237.
(11) Garcia-Araez, N.; Climent, V.; Feliu, J. Potential-dependent water orientation on Pt(111), Pt(100), and Pt(110), as inferred from laser-pulsed Experiments. Electrostatic and chemical effects. *J. Phys. Chem. C* **2009**, *113*, 9290−9304.
(12) García-Aráez, N.; Climent, V.; Feliu, J. M. Potential-dependent water orientation on Pt(111) stepped surfaces from laser-pulsed experiments. *Electrochim. Acta* **2009**, *54*, 966−977.
(13) Sebastián, P.; Martínez-Hincapié, R.; Climent, V.; Feliu, J. M. Study of the Pt(111) | electrolyte interface in the region close to neutral pH solutions by the laser induced temperature jump technique. *Electrochim. Acta* **2017**, *228*, 667−676.
(14) Clavilier, J.; Orts, J. M.; Gómez, R.; Feliu, J. M.; Aldaz, A. *Electrochemical Society Proceedings*, vol. 94−21. The Electrochemical Society, Pennington, NJ, pp 167−184.
(15) Lucas, C. A.; Markovic, N. M.; Ross, P. N. Adsorption of halide anions at the Pt(111)-solution interface studied by in situ surface x-ray scattering. *Phys. Rev. B: Condens. Matter Mater. Phys.* **1997**, *55*, 7964−7971.
(16) Garwood, G. A., Jr.; Hubbard, A. T. Superlattices formed by interaction of hydrogen bromide and hydrogen chloride with Pt(111) and Pt(100) studied by LEED, Auger and thermal desorption mass spectroscopy. *Surf. Sci.* **1981**, *112*, 281−305.
(17) Stickney, J. L.; Rosasco, S. D.; Salaita, G. N.; Hubbard, A. T. Ordered ionic layers formed on platinum(111) from aqueous solutions. *Langmuir* **1985**, *1*, 66−71.
(18) Salaita, G. N.; Stern, D. A.; Lu, F.; Baltruschat, H.; Schardt, B. C.; Stickney, J. L.; Soriaga, M. P.; Frank, D. G.; Hubbard, A. T. Structure and composition of a platinum(111) surface as a function of pH and electrode potential in aqueous bromide solutions. *Langmuir* **1986**, *2*, 828−835.
(19) Lucas, C. A.; Markovic, N. M.; Ross, P. N. Observation of an ordered bromide monolayer at the Pt(111)- solution interface by in-situ surface X-ray scattering. *Surf. Sci.* **1995**, *340*, L949−L954.
(20) Gasteiger, H. A.; Markovic, N. M.; Ross, P. N. Bromide adsorption on Pt(111): Adsorption isotherm and electrosorption valency deduced from RRD(Pt(111))E measurements. *Langmuir* **1996**, *12*, 1414−1418.
(21) Orts, J. M.; Gómez, R.; Feliu, J. M.; Aldaz, A.; Clavilier, J. Voltammetry, charge displacement experiments, and scanning tunneling microscopy of the Pt(100)-Br system. *Langmuir* **1997**, *13*, 3016−3023.
(22) Garcia-Araez, N.; Climent, V.; Herrero, E.; Feliu, J.; Lipkowski, J. Thermodynamic studies of bromide adsorption at the Pt(111) electrode surface perchloric acid solutions: Comparison with other anions. *J. Electroanal. Chem.* **2006**, *591*, 149−158.
(23) Tanaka, S.; Yau, S. L.; Itaya, K. In-situ scanning tunneling microscopy of bromine adlayers on Pt(111). *J. Electroanal. Chem.* **1995**, *396*, 125−130.
(24) Bertel, E.; Schwaha, K.; Netzer, F. P. The adsorption of bromine on Pt(111): Observation of an irreversible order-disorder transition. *Surf. Sci.* **1979**, *83*, 439−452.
(25) Korzeniewski, C.; Climent, V.; Feliu, J. M. Electrochemistry at Platinum Single Crystal Electrodes. *Electroanalytical Chemistry: A Series of Advances* **2011**, *24*, 75−170.
(26) Clavilier, J.; Armand, D.; Sun, S. G.; Petit, M. Electrochemical adsorption behaviour of platinum stepped surfaces in sulphuric acid solutions. *J. Electroanal. Chem. Interfacial Electrochem.* **1986**, *205*, 267−277.
(27) Climent, M. A.; Valls, M. J.; Feliu, J. M.; Aldaz, A.; Clavilier, J. The behavior of platinum single-crystal electrodes in neutral phosphate buffered solutions. *J. Electroanal. Chem.* **1992**, *326*, 113−127.
(28) Gisbert, R.; García, G.; Koper, M. T. M. Adsorption of phosphate species on poly-oriented Pt and Pt(111) electrodes over a wide range of pH. *Electrochim. Acta* **2010**, *55*, 7961−7968.
(29) Briega-Martos, V.; Herrero, E.; Feliu, J. M. Effect of pH and water structure on the oxygen reduction reaction on platinum electrodes. *Electrochim. Acta* **2017**, *241*, 497−509.
(30) Chen, X.; McCrum, I. T.; Schwarz, K.; Janik, M. J.; Koper, M. T. M. Co-adsorption of cations as the cause of the apparent pH dependence of hydrogen adsorption on a stepped platinum single-crystal electrode. *Angew. Chem., Int. Ed.* **2017**, *56*, 15025−15029.
(31) Yaguchi, M.; Uchida, T.; Motobayashi, K.; Osawa, M. Speciation of adsorbed phosphate at gold electrodes: A combined surface-enhanced infrared absorption spectroscopy and DFT study. *J. Phys. Chem. Lett.* **2016**, *7*, 3097−3102.
(32) Garcia-Araez, N.; Climent, V.; Herrero, E.; Feliu, J. M.; Lipkowski, J. Thermodynamic approach to the double layer capacity of a Pt(111) electrode in perchloric acid solutions. *Electrochim. Acta* **2006**, *51*, 3787−3793.
(33) Garcia-Araez, N.; Climent, V.; Rodriguez, P.; Feliu, J. M. Elucidation of the chemical nature of adsorbed species for Pt(111) in H_2SO_4 solutions by thermodynamic analysis. *Langmuir* **2010**, *26*, 12408−12417.
(34) Climent, V.; Attard, G. A.; Feliu, J. M. Potential of zero charge of platinum stepped surfaces: a combined approach of CO charge displacement and N2O reduction. *J. Electroanal. Chem.* **2002**, *532*, 67−74.
(35) Weaver, M. J. Potentials of zero charge for platinum(111)-aqueous interfaces: A combined assessment from in-situ and ultrahigh-vacuum measurements. *Langmuir* **1998**, *14*, 3932−3936.
(36) Climent, V.; Garcia-Araez, N.; Herrero, E.; Feliu, J. Potential of zero total charge of platinum single crystals: A local approach to stepped surfaces vicinal to Pt(111). *Russ. J. Electrochem.* **2006**, *42*, 1145−1160.
(37) Attard, G. A.; Hazzazi, O.; Wells, P. B.; Climent, V.; Herrero, E.; Feliu, J. M. On the global and local values of the potential of zero total charge at well-defined platinum surfaces: stepped and adatom modified surfaces. *J. Electroanal. Chem.* **2004**, *568*, 329−342.
(38) Martinez-Hincapie, R.; Sebastian-Pascual, P.; Climent, V.; Feliu, J. M. Investigating interfacial parameters with platinum single crystal electrodes. *Russ. J. Electrochem.* **2017**, *53*, 227−236.
(39) Garcia-Araez, N.; Climent, V.; Herrero, E.; Feliu, J. M.; Lipkowski, J. Determination of the Gibbs excess of H adsorbed at a Pt(111) electrode surface in the presence of co-adsorbed chloride. *J. Electroanal. Chem.* **2005**, *582*, 76−84.

DOI: 10.1021/acs.jpcc.8b05685
J. Phys. Chem. C 2018, 122, 18562−18569